Article

Not peer-reviewed version

# Petrophysical and Mechanical Properties of the Piromafo Stone Used in the Built Heritage of Apulia (SE Italy): A Comprehensive Laboratory Study

Gioacchino Francesco Andriani *

Posted Date: 11 June 2024

doi: 10.20944/preprints202406.0669.v1

Keywords: Pietra Leccese; fabric; hydraulic behaviour; thermal properties; strength; weathering

 doi:10.20944/preprints202406.0669.v1



*Article*

# Petrophysical and Mechanical Properties of the *Piromafo* Stone Used in the Built Heritage of Apulia (SE Italy): A Comprehensive Laboratory Study

**Gioacchino Francesco Andriani** [1,*]

Dipartimento di Scienze della Terra e Geoambientali, Università degli Studi di Bari ALDO MORO, Via Edoardo Orabona 4, 70125, Bari, Italy; gioacchinofrancesco.andriani@uniba.it

**Abstract:** Many historic buildings and monuments on the Salento Peninsula (Apulia, southern Italy) were built from locally quarried Miocene calcarenites belonging to the Pietra Leccese Formation (Late Burdigalian-early Messinian). The main facies consists of a homogeneous and porous biomicrite, pale yellow in color and fine- to medium-grained, very rich in planktonic Foraminifera and massive or thick-bedded in outcrop. Additionally, there are other facies among which *Piromafo* stands out for its aesthetic appearance, which is enhanced by its greenish-brown or greenish-grey colors. Its physical characteristics, in terms of thermal properties mainly due to the mineral content and fabric, make it a good refractory and insulation material. *Piromafo* occurs in the upper part of the Pietra Leccese Fm. and is represented by a fine- to medium-grained glauconitic and phosphatic biomicrite with macrofossils, especially Bivalves and Gastropods. Despite its important historical use as building and ornamental material, especially in the Roman and Baroque architecture, a research gap exists in the scientific literature describing the properties of the stone and their correlation. Therefore, the aim of this paper is to present a wide range of properties useful to explain the in-situ behavior and damage susceptibility of the stone in monuments and buildings, but also for selecting preservation treatments and strategies. Thus, an overall assessment of the main petrophysical and mechanical properties especially for restoration/conservation purposes was performed using both standard and unconventional techniques. Starting from rock fabric inspection, particular attention was given to the relationship be-tween pore-size distribution and, hydraulic and thermal properties of the material. Unconfined compressive strength, flexural strength and indirect tensile strength were also estimated.

**Keywords:** Pietra Leccese; fabric; hydraulic behaviour; thermal properties; strength; weathering

## 1. Introduction

The Salento area, in particular the city of Lecce (Apulia, southern Italy), is very famous for the splendor of its 17th–18th c. Baroque architecture characterized by the use of stones derived from the Pietra Leccese Fm. (Late Burdigalian-early Messinian) which crops out locally throughout the area [1–4]. The Pietra Leccese Fm. is comprised mainly of a white-yellowish, fine-grained, calcarenite. It is a hemipelagic chalk-like carbonate, homogeneous and porous with a wackestone/packstone depositional texture, composed of calcareous microfossils, such as Foraminifera, and bioclasts of Bivalves, Ostracods, Echinoderms and pellets. Additional allochems also include intraclasts. Within this unit, different lithofacies alternate both vertically and laterally, constituting many varieties which are identified with traditional local building stone, names such as: *Mazzara, Leccisu, Pietra bastarda, Dura, Bianca, Dolce, Gagginara, Piromafo, Cucuzzara, Saponara* and *Niura*. These stone varieties differ considerably in color and stone pattern, as well as physical and mechanical performance which are strongly dependent on depositional fabric and, degree and type of diagenesis. At the same time, the material durability, defined as the property of natural building stone to resist the weathering agents

 doi:10.20944/preprints202406.0669.v1



in the course of time and preserve its appearance and characteristics of strength, is not the same in the different varieties.

*Piromafo* (*Pirómafo* or *Pirómaco*) is a phosphatic-glauconitic biomicrite rich in plancktonic Foraminifera. It is characterised by its greenish-brown or greenish-grey colours and stone pattern due to the presence of macrofossils, at places, concentrated in some levels [5]. Its name comes from the ancient Greek πῦρ (fire) combined with the verb μάχομαι (fight), which reflects its good refractory and thermal insulation properties [6]. Today, in fact, due to its high thermal resistance, it is suitable for the furnishing of fireplaces, hearths, ovens, kilns and chimneys, while the historical use of this material is much more interesting, especially from the Roman times (Figure 1) and Baroque period. The well-known Baroque Convent of Agostiniani (1573-1662), at Melpignano (South of Salento), and the monumental pier of San Cataldo (Lecce), the main coastal harbour of the Roman town of Lupiae, are just two examples [7]. The outcrops of *Piromafo* are numerous even if limited in thickness (few meters) and include the areas of Novoli and Surbo to the North of Lecce, Vernole, Vanze, Strudà, Acaya, and Pisignano to the South-East of Lecce, and Cursi, Melpignano, Martano, Zollino, and Poggiardo to the South of Salento (Figure 2).

**Figure 1.** The Roman Pier of San Cataldo (2nd century A.D.) at Lecce, Adriatic coast of Apulia (SE Italy).

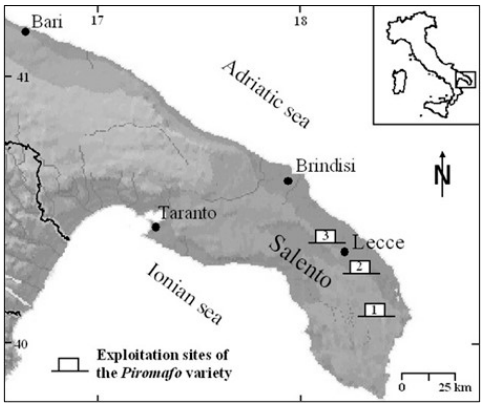


**Figure 2.** Geographic location of the main extraction areas of the Piromafo variety: **1**) Cursi, Melpignano, Martano, Zollino, and Poggiardo; **2**) Vernole, Vanze, Strudà, Acaya, and Pisignano; **3**) Novoli and Surbo.

The purpose of this work is to present a comprehensive review of the main petrophysical and mechanical properties of the *Piromafo* stone given the absence in the literature of a complete characterization of this material. From the comprehensive literature review presented and discussed in this study, in fact, it is possible to state that the existing research done since the past century on *Piromafo* has been focused on the geo-stratigraphic and mineralogical features, leaving aside

 doi:10.20944/preprints202406.0669.v1



information concerning technical properties and durability, in spite of its predisposition to weathering and carsogenesis [8].

Thus, studies addressing different technical aspects, especially in terms of hydraulic and thermal properties, constitute fundamental tools and knowledge for qualitative and quantitative performance assessment of the stone's resistance to weathering processes. This should be both significant and appealing, especially when the study method is innovative because it includes a multidisciplinary approach involving both standard and unconventional techniques.

Therefore, rock fabric inspection was performed by means of transmitted light on standard thin-sections using an optical polarizing microscope. Specific gravity, density, porosity, water absorption and degree of saturation were obtained following the test procedure described in the ISRM, ASTM and EN standards. Pore-size distribution was carried out by mercury intrusion Porosimetry (MIP) and image analysis (IA) performed on photomicrographs applying the methods of quantitative stereology. Computer analysis of digital images was applied to determine also the grain-size distribution. Water permeability tests were conducted on cylindrical rock samples using the falling head method. The thermal parameters were determined with the experimental "cut-core" method [9–11], first in the dry state and then in the saturated state.

Unconfined compressive strength, flexural strength, indirect tensile strength, Point Load index and Schmidt hammer rebound were calculated and compared. Particularly, compressive strength and tangent modulus were correlated with the Schmidt hammer rebound values.

## 2. Materials and Methods

Samples of the *Piromafo* stone were taken from the quarry districts of Strudà-Acaja (South-East of Lecce) and Cursi-Melpignano, along the road which connects Cursi to Melpignano (*Zezza* quarry, South Salento) where quarry walls carved in the Pietra Leccese Fm. expose *Piromafo* in outcrops about two meters thick. In both the sampling sites, the *Piromafo* facies is represented by a strongly glauconitic biomicrite, greenish or greenish-brown in the upper part and greenish-grey, massive beds very rich in bivalves (mainly pectinids) in the lower part (Figure 3). The green and brown grains are respectively glauconitic and phosphatic, apatitic nodules (a few millimetres to 2-3 cm in size), which at places, are concentrated in decimeter thick dark green lenses. Therefore, the different greenish shades of the outcrops are attributable to the presence of glauconite and apatite and depend on the degree of crystallization or alteration of glauconite and the percentage of phosphates present [12,13]. At the Cursi-Melpignano sites, two lenses of about 0.3 meters thick are characterized by a wavy pattern with such a high concentration of apatite nodules and macrofossils (Bivalves) which the local quarrymen call *mussel levels* [14]. The glauconite biomicrites show a gradually change up-section due to the decrease of the glauconitic content and the increase in the carbonate component resulting in a graded contact with the overlying Calcareniti di Andrano Fm. (Messinian). Patterns of bioturbation can be observed, especially where the concentrations in fossil bivalve shells is higher (mainly at Strudà-Acaja site). These are, mainly, horizontal burrowing trace fossils.

The origin of glauconite is controversial and lacks a consensus of views and interpretations regarding all the chemical reactions and the parameters that control the development of the mineral. Some authors, in fact, believe that glauconite is not an environmental indicator. They provide evidence that it has been found in both tidal-sea and deep-sea sediments of low sedimentation rate [15–20]. The apatite grains are detrital in origin and derive from the erosion of pre-existing sediments that included phosphate levels of variable percentages depending on the biogenic or terrigenous nature of the original clasts [21,22].

 doi:10.20944/preprints202406.0669.v1



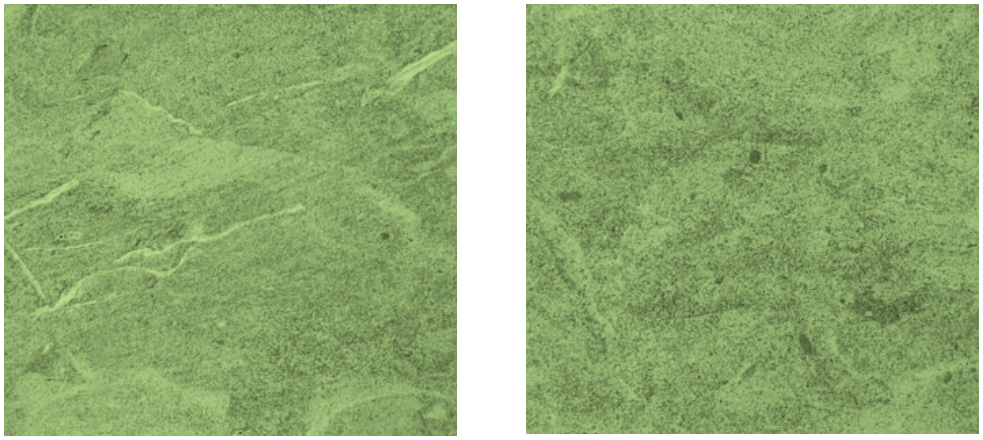

(**a**) (**b**)

**Figure 3.** This Mesoscopic appearances of the Piromafo specimens respectively from Strudà-Acaja (**a**) and Cursi-Melpignano (**b**).

Evaluating physical and mechanical properties of stones used as building and ornamental material is an interesting and complex challenge due to the often encountered need to adapt, modify or implement the methods and techniques described in international standards to the characteristics l.s. of materials, especially in terms of rock composition and fabric, with respect to the purposes of investigation. For this study, a multidisciplinary approach using traditional methods of investigation associated with new experimental unconventional techniques was used. Therefore, polarized optical microscopy and image analysis (IA) on microphotos coupled with mercury intrusion porosimetry technique (MIP) and basic geotechnical testing were used to classify the materials and their pore structures. According to ASTM [40], a chemical analysis of samples crushed and powdered by mechanical method with porcelain mortars and pestles was performed.

Furthermore, block samples were collected during the field investigation and then transferred to the Geotechnical Laboratory at the Department of Earth and Environmental Science, ALDO MORO University of Bari (Italy). Testing specimens were prepared in five shapes: irregular, cylinder, square bar or slab, disc and cubic. Standard tolerance limits for linear measures were adopted with an accuracy of 0.1 mm, as required by EN [23]. Physical and mechanical properties were determined on 95 samples (44 samples from the Strudà-Acaja and 51 samples from the Cursi-Melpignano areas), which enabled mutual correlation of values. Irregular specimens were used for thin sections, mercury intrusion porosimetry (MIP) and the Point Load test (PLT). Cylindrical specimens (diameter of 71 mm and height of 140 mm) were used for the water permeability test and thermal conductivity measurements. Square bars (length of 350 mm, height of 15 mm, width of 15 mm) were used for the thermal linear expansion test. Square tile specimens (length of 300 mm, height of 50 mm, width of 50 mm) were used to conduct the flexural strength test and disc specimens (diameter of 54 mm, height to diameter ratio was 0.5:1) were prepared from cylinder specimens and used for the indirect tensile strength test (Brazilian test). Cubic specimens (80 mm in length) were used for Schmidt hammer and unconfined compressive strength (UCS) tests. Hygrometric and capillary properties were evaluated on the cubic specimens, successively saturated under vacuum and used also for UCS tests. Density measures were performed on all the samples of regular geometric shape.

Following the standard test procedures outlined in ISRM [24–27] and EN [28–30], specific gravity ($G_s$), dry density ($\varrho_d$), saturated density ($\varrho_{sat}$), total porosity (n), unconfined compressive strength in the dry ($\sigma_n$) and saturated state ($\sigma_{sat}$), flexural strength ($\sigma_f$) and tensile strength in the dry state (($\sigma_t$) were determined. For the UCS test, a group of 30 samples (14 from the Strudà-Acaja and 16 from the Cursi-Melpignano areas) were used half in the dry state and half in the saturated state. Stress-strain curves were obtained by estimating the stress with a pressure transducer and the axial displacement with an LVTD sensor; lateral displacement was not recorded. The modulus of elasticity was derived from the UCS test on dry samples from the slope of the stress-strain curves by tangent modulus (Et).

 doi:10.20944/preprints202406.0669.v1



A group of 12 samples (6 both from the Strudà-Acaja and the Cursi-Melpignano areas) was used respectively for flexural strength and tensile strength in the dry state. It was not possible to perform all the mechanical tests both in the dry and saturated state due to lack of material.

According to Andriani and Walsh [31,32] water absorption ($w_a$) and degree of saturation (Sr) were evaluated on 12 specimens (6 both from the Strudà-Acaja and the Cursi-Melpignano areas) immersed and suspended in distilled water at 20°C for 48 h and then saturated completely under vacuum (80 kPa) without removing them from the water basket. Specific Gravity was determined (5 samples from both the Strudà-Acaja and the Cursi-Melpignano areas) by measuring the grain volume with the pulverization method by displacement of an equivalent volume of distilled water in a pycnometer. The MIP tests were carried out as outlined by ASTM [33] on 6 oven-dried samples of about 2.5 g (3 from both the Strudà-Acaja and the Cursi-Melpignano areas). A Micromeritics AutoPore IV 9500 porosimeter was used at low (3.44–345 kPa) and high pressure (0.1–228 MPa), both in intrusion and in extrusion, covering pore diameters between 420 and 0.005 μm, approximately. In particular, total pore area, average pore diameter, pore-size distribution, complementary measures of porosity ("effective" porosity), tortuosity and permeability were evaluated. The results of the MIP test were integrated with the pore-size distribution obtained by image analysis on microphotographs of thin sections, according to the procedure proposed by Andriani and Walsh [31], and Andriani et al. [34]. Water permeability tests were conducted with a purpose-built cell using the falling head method according to the procedure proposed by Andriani and Walsh [32]. A group of 10 cylindrical specimens (4 from the Strudà-Acaja and 6 from the Cursi-Melpignano areas) were used for this test. The hydraulic conductivity standardized at 20°C ($k_{20}$) was evaluated for a range of hydraulic gradients between 0.5 and 15. The thermal properties of *Piromafo* were obtained from the measurement of the thermal linear expansion coefficient ($\alpha_l$), based on mechanical length-change measurements at 20, 40, 60 and 80°C according to EN [35]. For these measurements, 4 and 7 square bar samples were prepared respectively for the Strudà-Acaja and the Cursi-Melpignano areas. The thermal conductivity ($\lambda$) in variable regime was obtained on 4 specimens for each study site by means of the experimental "cut-core" method [9–11,36]; measurements were taken on the same samples first in the dry state and then in the saturated state. The hygroscopic sorption properties of the material were carried out through the equilibrium moisture content measured using the desiccator method as specified in EN ISO [37] on 14 cubic specimens (7 from both the Strudà-Acaja and the Cursi-Melpignano areas) in equilibrium with air at the specific temperature of 21±1°C and relative humidity (RH) of 61±2%. The test ended when the weight of the specimens became stable, specifically after 4 days. The capillary water absorption coefficient (Aw) was estimated according to EN [29] at the specific temperature of 21±1°C and relative humidity (RH) of 52±2%, with the tangent method by plotting the cumulative mass of water absorbed per unit area against the square root of time.

Schmidt hammer tests were performed on the same cubic samples employed for the UCS test using an L-type instrument according to Aydin [38]. The rebound values (thirty for each block, five measures on every face) obtained in vertical downwards impact directions were normalized using the correction curves provided by the manufacturer. According to the ISRM [39], the Point Load test was performed on 5 irregular lumps for each study site and the uncorrected Point Load Strength Index (Is) was recalculated to the Size-corrected Point Load Strength Index Is (50) which corresponds to the standard core diameter of 50 mm. By comparing and combining analysis of the experimental results with literature data and information, a critical assessment of petrophysical and mechanical properties of the material was carried out, suitable for deriving relationships between the different parameters considered in this study and evaluating its susceptibility to weathering.

## 3. Results

### *3.1. Material Classification*

Rock fabric examination was performed with transmitted light on standard thin-sections using an optical polarizing microscope. Thin-sections were taken from specimens at orthogonal orientations, half were cut parallel (two for each study site) and half at right angles (two for each

 doi:10.20944/preprints202406.0669.v1



study site) to the quarry walls (Figure 4). The *Piromafo* reveals homogeneous minero-petrographic characteristics and is almost exclusively formed from low-Mg CaCO3 (about 90%). A much lower quantity of glauconite, apatite and rare quartz grains are present, as well as clayey minerals finely distributed in the matrix with a carbonate composition. In fact, *Piromafo* records the maximum insoluble residue content (12%) among the varieties of the Pietra Leccese Fm. [22]. Two types of glauconite granules are recognized, one of green colour mostly concentrated in layers, the other of yellowish colour, finely dispersed in the matrix. Previous studies have shown that these are granules of glauconite with different chemical composition varying in the content of $SiO_2$ and $Fe_2O_3$ (47.09 % and 24.07 % for the green glauconite and, 28.88 % and 46.36 % for the yellowish glauconite, respectively) [12].

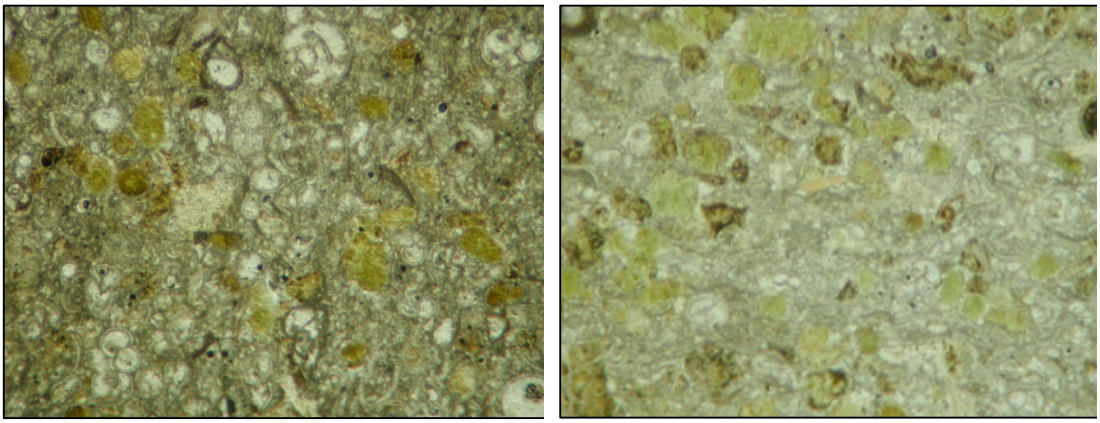

(**a**) (**b**)

**Figure 4.** Microphotographs in plane-polarized light from thin sections of the Piromafo: microscopic appearances of samples respectively from Strudà-Acaja (**a**) and Cursi-Melpignano (**b**). The length of view field for each photo is 2 mm.

The general fabric is one of a tightly packed and fine-grained calcarenite, with a self-supporting framework of skeletal grains of marine organisms (mostly, planktonic Foraminifera and, to a lesser extent, benthic Foraminifera and rare Lamellibranchs and Echinoderms), fossil debris and pellets. The typical grains are rounded to subrounded and range in size between 0.25-0.50 mm. Two pellet types were recognized: small clay pellets in the matrix and larger heterogeneous pellets, green to black, compacted ovoids that are easily observable. The microcrystalline calcite matrix (micrite) is not diffuse; it is dark coloured and forms a predominantly cryptocrystalline based mass or thin envelopes around skeletal grains (microforaminifera, Bivalves, and Gastropods) not always resolvable by polarizing microscopy. Sparry calcite occurs as pore filling cement and is distinguished from micrite by its clarity as well as coarser crystal size, which may range up to 20 micrometers. On the basis of the pore types and porosity classification of carbonate rocks proposed by Choquette and Pray [41], the greatest contribution to the total porosity is provided by the intergranular porosity, but the moldic porosity by dissolution of aragonite bioclasts and intragranular porosity, essentially linked to the internal structures of Foraminifera, are also effective at the microscopic scale. Isolated porosity, linked to the closed interstices is uncommon. Microfracture porosity characterizes, at places, the samples coming from Strudà-Acaja, as with intercrystal porosity which is typical of rock sections showing the effects of recrystallization and/or neomorphic processes. The majority of the samples reveal grain-supported fabric, mainly packstone according to Dunham [42]. They are, principally, packed biomicrites (Strudà-Acaja) or poorly washed biosparites (Cursi-Melpignano), according to Folk [43]. They are well sorted to moderately well-sorted due to the presence of Bivalve shell fragments.

 doi:10.20944/preprints202406.0669.v1



*3.2. Physical and Mechanical Properties*

According to the test results (Table 1), there is no significant variation of physical and mechanical properties among the tested samples coming from the same study site, but it is possible to observe small differences between the samples coming from the two different areas. The average values were used to make a comparative analysis and highlight relationships between the properties of the materials.

**Table 1.** Physical and mechanical properties of the *Piromafo* stone.

| **Physical-Mechanical Properties** | **Extraction sites of the *Piromafo*** | |
|---|---|---|
| | Strudà-Acaja | Cursi-Melpignano |
| Specific gravity, $G_s$ | 2.72 – 2.75 | 2.70 – 2.75 |
| Dry density, $\varrho_d$ (Mg/m$^3$) | 1.60 – 1.73 | 1.64 – 1.71 |
| Sat. density, $\varrho_{sat}$ (Mg/m$^3$) | 2.00 – 2.11 | 2.07 – 2.10 |
| Total porosity, n (%) | 37 – 42 | 35 -40 |
| Water absorption, $w_a$ (%) | 20 – 26 | 20 – 24 |
| Degree of saturation, Sr (%) | 97 – 100 | 95 – 100 |
| Hygroscopic moisture content, $w_h$ (%) | 0.5 – 0.8 | 0.6 – 0.8 |
| Capillary water absorption Coeff., $A_w$ (mg/cm$^2$ s $^{1/2}$) | 8.8 – 9.2 | 10.6 – 11.1 |
| Hydraulic conductivity (Falling head test), $k_{20}$ ($10^{-5}$ m/s) | 0.5 – 7.8 | 0.8 – 7.2 |
| Thermal linear expansion, $\alpha_l$ ($10^{-6}$ K$^{-1}$) | 3.07 – 3.51 | 3.34 – 3.87 |
| Thermal conductivity (dry),$\circledcirc_d$ (W m$^{-1}$K$^{-1}$) | 0.62 – 0.73 | 0.64 – 0.76 |
| Thermal conductivity (sat), $\circledcirc_{sat}$ (W m$^{-1}$K$^{-1}$) | 0.84 – 1.13 | 0.82 – 1.19 |
| Compr. Strength (dry), $\circledcirc_n$ (MPa) | 13.2 – 15.1 | 13.8 – 16.7 |
| Tangent Modulus (dry), $E_t$ (GPa) | 3.6 – 5.5 | 4.1 – 6.7 |
| Compr. strength (sat), $\circledcirc_{sat}$ (MPa) | 6.8 – 8.4 | 7.1 – 8.8 |
| Flexural strength (dry) $\circledcirc_f$ (MPa) | 1.8 – 3.1 | 2.1 – 3.4 |
| Indirect Tensile strength (dry), $\circledcirc_t$ (MPa) | 1.1 – 2.2 | 1.4 – 2.2 |
| Point Load Test index (dry), $I_{S(50)}$ (MPa) | 1.3 – 1.7 | 1.2 – 1.9 |
| Schmidt Rebound Number (dry), $R_l$ | 14 – 20 | 14 – 20 |

## 4. Discussion

According to rock type classification of The Geological Society of London [44], *Piromafo* is a medium/fine-grained calcarenite with a pore network constituted, almost in its entirety, of capillary pores smaller than 4 μm (Figure 5). The MIP measures give interesting information not only about the volume of open voids, but also about pore shape and size, thus providing an important tool to understand the contribution of porosity and the 3D pore system with respect to the material's durability [45].

 doi:10.20944/preprints202406.0669.v1



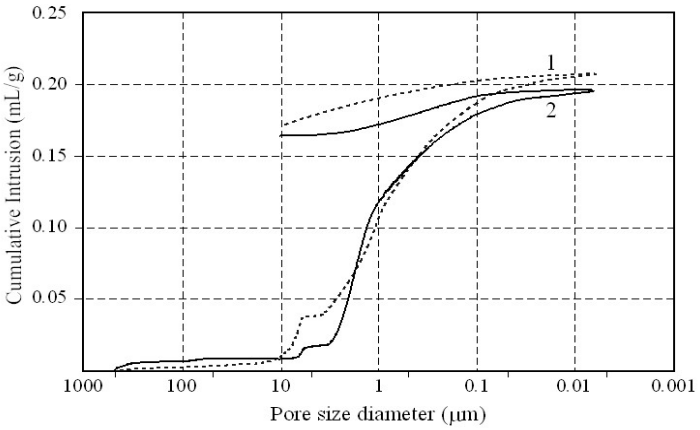


**Figure 5.** Cumulative intrusion/extrusion curves as a function of pore diameter measured by mercury intrusion porosimetry (MIP) for two samples from the two extraction areas: **1**) Cursi-Melpignano; **2**) Strudà-Acaja.

Comparing the results obtained for the two sites, it can be noted that the Cursi-Melpignano samples show a more marked presence of large and medium capillary pores, sensu Mindess [46] and a minor presence of entrained air pores (> 75 μm), probably linked to microcraks (through pores). In fact, from the extrusion curves, it is possible to state that for Cursi-Melpignano samples the presence of bottle-neck pores is more remarkable. Indeed, the tortuosity factor is, on average, 1.34 for Strudà-Acaja and 1.85 Cursi-Melpignano.

In this study, the pore-size distributions obtained by MIP are very similar to those found by other authors for different facies belonging to the Pietra Leccese Fm. [47–49], but with a higher and slightly wider pore-size distribution around the modal class of 2-4 microns. Furthermore, the pore-size distributions obtained from a combination of porosimetry results and image and textural analysis results, according to the method proposed by Andriani and Walsh [31] and Andriani et al. [34], demonstrate that the Strudà-Acaja samples have a greater presence of pores greater than 63 μm, intragranular and microfracture in type, above all controlled by fossils and microcracks (Figure 6). Thus, as has been shown by Andriani et al. [34] for other calcarenite lithofacies cropping out in Apulia (eg. Calcarenite di Gravina Fm.), also as regards the pore structure of the *Piromafo* stone it is possible to affirm the existence of a dual porosity which influences its hydraulic behaviour in terms of such properties as capillarity, water absorption and water flow in unsaturated and saturated conditions.

The specific gravity average value is 2.73 and 2.72 for the samples from Strudà-Acaja and Cursi-Melpignano, respectively; these values are on average higher than the classic one for Apulian carbonates (2.70) due especially to the presence of apatite nodules and glauconite granules with high iron content. The dry density average value is 1.67 Mg/m$^3$ and 1.69 Mg/m$^3$ for the samples from Strudà-Acaja and Cursi-Melpignano, respectively; it is therefore midway between soft and medium hard rocks.

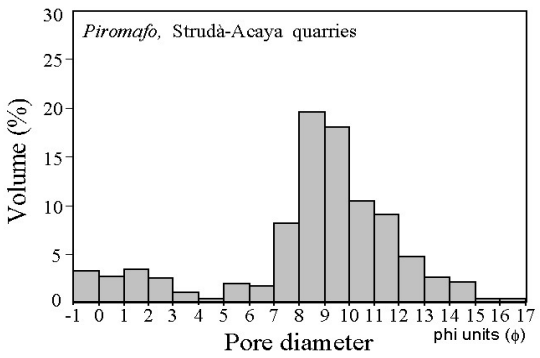


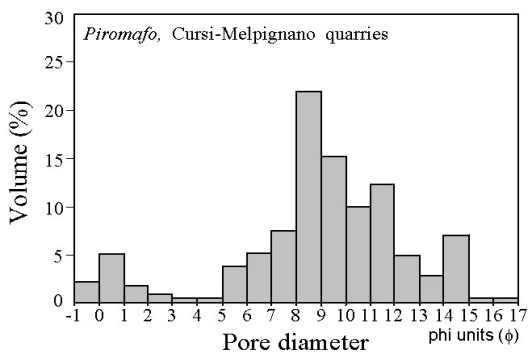

 doi:10.20944/preprints202406.0669.v1



(**a**) (**b**)

**Figure 6.** Pore-size distribution obtained from combination of the MIP results and, image and textural analysis, according to the method proposed by Andriani and Walsh [31] and Andriani et al. [34]. **a**) Strudà-Acaja. **b**) Cursi-Melpignano;.

According to the total porosity average values (39% and 37% respectively for Strudà-Acaja and Cursi-Melpignano), those of total water absorption (24% and 22% respectively for Strudà-Acaja and Cursi-Melpignano) and those of degree of saturation (98% in both cases), the material has high total porosity which can be considered, mainly, an effective porosity. It follows that when the material is completely submerged, it absorbs a great proportion of water because the greatest part of pores in the rock particle systems are interconnected and continuous. The *Piromafo* samples adsorbed around 80% of the total absorbed water in the first 20 minutes of the testing, afterwards, the absorption of water slowly increases, up to the maximum. Hygroscopic moisture content is on average equal for the samples of the two sites. It is 0.7 % with a degree of saturation between 3.2 % and 3.7 %. The higher values characterize the samples coming from Cursi-Melpignano, probably due to a greater presence of hygroscopic minerals, such as glauconite, sulphates and clay minerals, the latter as very fine grains attached to micrite matrix. It is important to emphasize that the hygroscopic water varies with the relative humidity and temperature of the environment. The absorption of water due to capillary forces is on average higher for the samples from Cursi-Melpignano. This is a consequence of a greater presence of capillary pores (< 5 μm, sensu Mehta and Monteiro [50]) and pores open only at one end, and a lesser presence of macropores with respect to the samples from Strudà-Acaja. The capillary water absorption coefficient is found to be on average 9.0 and 10.8 mg/cm² s ½ respectively for the samples from Strudà-Acaja and Cursi-Melpignano. All samples exhibit first stage curves defined by a straight line. As a result, calculation of the capillary water absorption coefficient by the tangent method according to EN [29] is more easily achieved (Figure 7).

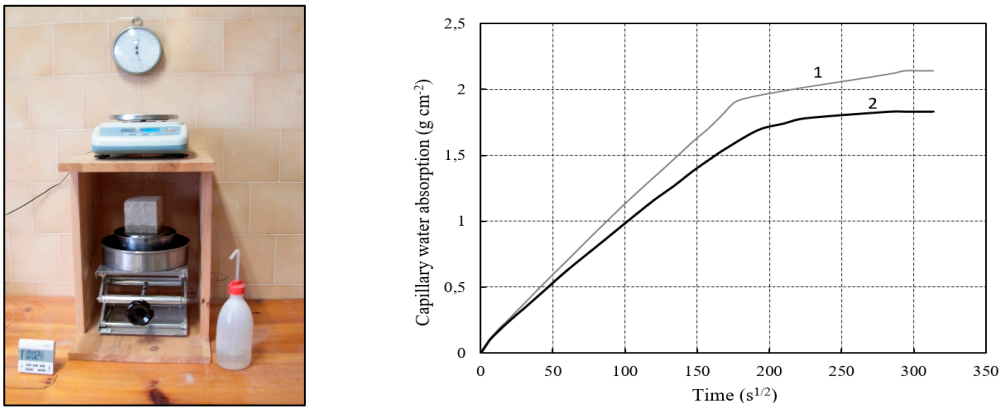


(**a**) (**b**)

**Figure 7.** Capillary water absorption experimental device (**a**) and results (**b**): **1**) Cursi-Melpignano; **2**) Strudà-Acaja.

In the falling head test, the hydraulic conductivity measurements are found to be approximately between $10^{-5}$ and $10^{-6}$ m/s for the two varieties studied; the ranges of data measured reveal overall a moderate water permeability for the *Piromafo*. The range of the hydraulic conductivity values is strongly conditioned by the presence of macrofossils and other discontinuities such as microfractures or other structural features. The evidence of a wider range of values with respect to other varieties of the Pietra Leccese Fm. is thus attributed to the effects of secondary permeability which provide rapid fluid transfer across the material, although at the sample scale secondary permeability does not always occur. Furthermore, the presence of glauconite, as well as clayey minerals finely distributed in the micrite matrix, decreases the material's capacity to transmit water, thereby increasing the time of residence of water within the material. Not surprisingly, an insoluble residue content of about 12%

 doi:10.20944/preprints202406.0669.v1



was calculated for the *Piromafo* stone. This is consistent with the observation that, other factors being equal, the samples that appeared more cemented, continuous and homogeneous showed the lowest values of the hydraulic conductivity. Additionally, *Piromafo*, compared to the other varieties of the Pietra Leccese Fm. [47,48] shows a wider distribution of pores and more pronounced dual porosity. Thus, the weathering susceptibility of *Piromafo* could be linked to its wider pore-size distribution, which, as shown in Figure 6, includes a large number of pores smaller than 30 μm connected by pore channels and throats to larger pores. These larger pores enhance water infiltration into the material, while the smaller pores retain water by capillary forces against drainage forces. The longer the water remains inside the material, the greater the effects of stone decay are.

With respect to the thermal properties, no substantial differences were observed between the samples from the two sites. The thermal linear expansion is found to be on average 3.38 and 3.75 $10^{-6}$ $K^{-1}$. The thermal conductivity in the dry state is on average 0.67 and 0.68 W $m^{-1}$ $K^{-1}$, while the thermal conductivity in the saturated state is on average 0.92 and 0.98 W $m^{-1}K^{-1}$, respectively for the samples from Strudà-Acaja and Cursi-Melpignano. It is possible to observe how the substitution in the pore system of air with water caused an increase in thermal conductivity.

A further consideration is that *Piromafo* shows a lower capability to conduct and propagate heat with respect to other varieties of the Pietra Leccese Fm. [4,36]. This feature can be attributable to the chemical and mineralogical composition of the material in its insoluble residue content rather than to the differences of porosity and pore network topology, taking into account that the total porosity is quite similar for all the varieties of the Pietra Leccese Fm., although the distribution of the pores can be different.

The uniaxial compressive strength and elastic modulus of the material at the dry state are found to be on average 14.1 and 15.0 MPa, and 4.7 and 5.5 GPa, respectively for the samples from Strudà-Acaja and Cursi-Melpignano. According to ISRM [26], *Piromafo* is a weak rock (R2). The overall mechanical behavior shows elastic–brittle features. Elastoplastic–brittle behavior was observed only for some samples in saturated conditions, especially for the lithofacies from Strudà-Acaja.

Considering the engineering classification for intact rock by strength and deformation properties after Deere and Miller [51], *Piromafo* is characterised by a very low strength (E) and average modulus ratio (M). According to the classification of the Apulian calcarenites (AC) by strength and rock fabric features after Andriani and Walsh [4], *Piromafo* is a moderately soft rock (AC1). Complete stress-strain curves illustrate that *Piromafo* is a material with medium stiffness and medium brittleness (Figure 8).

The uniaxial compressive strength of the material in the saturated state, the flexural strength, the indirect tensile strength, the Point Load Test index and the Schmidt Rebound Number at the dry state are found to be on average 7.8 and 7.7 MPa, 2.5 and 2.8 MPa, 1.6 and 1.9 MPa, 1.5 and 1.6 MPa, and 16 and 18, respectively for the samples from Strudà-Acaja and Cursi-Melpignano. Therefore, the presence of water in the pores of the rock leads to a reduction of the compressive strength values on average of 47%, indicating that saturation decreases the surface energy of crack faces and enables dissolution processes, especially in neomorphic calcite microcrystals and clay minerals dispersed in the micrite matrix. Consequently, both the overall cementation and the friction between the granules decrease, as well as the rock strength and elastic modulus. In particular, for the samples from Strudà-Acaja and Cursi-Melpignano the loss of strength at the saturated state is respectively of 45 and 49%. This is probably due to the better ability of the Cursi-Melpignano samples to hold water and to a greater possibility of water loss from the macropores during the test for the samples from Strudà-Acaja. Similar information about significant loss of strength and increase in deformability modulus of other calcarenite types due to water saturation are available in literature [52–54, and references therein].

 doi:10.20944/preprints202406.0669.v1



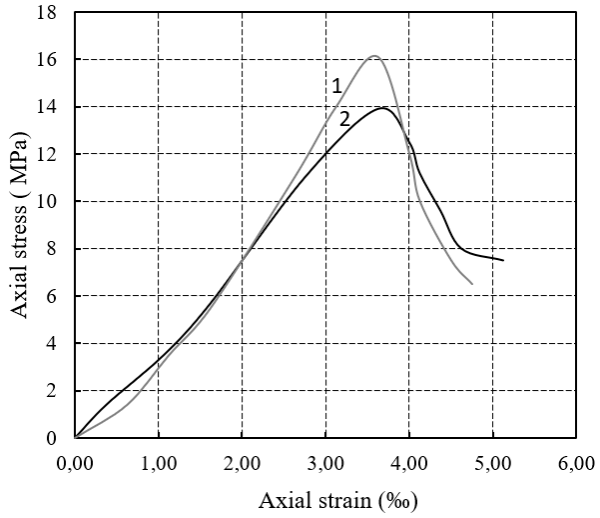


**Figure 8.** Typical stress–strain curves obtained for servo-controlled uniaxial compression tests on dry samples of the Piromafo variety: **1**) Cursi-Melpignano; **2**) Strudà-Acaja.

The ratio between uniaxial compressive strength, flexural strength and indirect tensile strength at the dry state is on average 5.5 and 8.4. The greater values of this ratio characterize the samples from Strudà-Acaja with values of 5.6 and 8.8, while values of 5.4 and 7.9 were found for the samples from Cursi-Melpignano. Generally, it can be said that the samples from Cursi-Melpignano are more resistant to flexural and tensile forces compared to those of Strudà-Acaja, but the differences are slight. The ratio between uniaxial compressive strength and the Point Load Test index at the dry state is on average 9.4 and 10, respectively for the samples from Strudà-Acaja and Cursi-Melpignano. The ratio between uniaxial compressive strength (MPa) and the Schmidt Rebound Number at the dry state are found to be on average 0.9 and 0.8, respectively for the samples from Strudà-Acaja and Cursi-Melpignano. Correlating the Schmidt hammer rebound values with compressive strength and tangent modulus for the Piromafo, the following power equations were obtained:

$$\sigma_n\,(MPa) = \ 3.7315\ R_L^{0.4907}\ with\ \ R^2 = 0.7662$$

$$E_t\,(GPa) = \ 0.1334\ R_L^{1.3047}\ with\ \ R^2 = 0.7046$$

These equations do not agree well with those obtained and presented by other researchers in the literature for both similar and different materials [38,39,55–60]. This evidence highlights the difficulty in finding relationships applicable to all carbonate rocks caused by the extreme variability and complexity of the fabric features which make the material anisotropic and affect its engineering behaviour.

Other correlations between mechanical properties were not considered statistically significant due to the limited data for some measurements.

## 5. Conclusions

In this work, *Piromafo*, a stone variety material derived from the Pietra Leccese Fm. was investigated, in terms of petrophysical and mechanical properties. Unfortunately, despite the historical use of this material, especially from the Roman times and the Baroque period, there exists very few references in the literature with a complete characterization of this material.

Destructive and non-destructive testing was used on samples taken from two extraction areas in the Lecce province (Apulia, southern Italy): 1) Strudà-Acaja; 2) Cursi-Melpignano. In particular, the study method was based on a multidisciplinary approach involving both standard and unconventional techniques.

 doi:10.20944/preprints202406.0669.v1



The attention was focused, especially, on fabric and mineral content influencing the thermal and hydraulic properties, weathering propensity and mechanical behaviour which are strongly controlled by the presence of water in pore spaces.

Some conclusions can be obtained as follows:

*i*) at the study sites, the *Piromafo* facies is represented, principally, by packed glauconitic biomicrites (Strudà-Acaja) and poorly washed glauconitic biosparites (Cursi-Melpignano), in which the total porosity (n) ranges from 37 to 42 % and from 35 to 40 % respectively. Determination of water absorption and degree of saturation on specimens completely immersed and suspended in distilled water under vacuum has shown that porosity for both the materials coming from the two study sites is almost all open with intercommunicating voids;

*ii*) the presence of both large and medium capillary pores and entrained air pores has demonstrated a wide pore-size distribution and dual porosity which can be responsible for the weathering susceptibility of the *Piromafo* stone;

*iii*) the experimental data demonstrated that the *Piromafo* stone is better as a refractory and heat insulation material with respect to other varieties of the Pietra Leccese Fm. and this is due to the chemical and mineralogical composition of the insoluble residue content (12%), which is comprised of glauconite, apatite, rare quartz grains and clayey minerals finely distributed in the matrix, rather than to the differences of total porosity, pore network topology and pore-size distribution;

*iv*) the results obtained from mechanical testing allowed the acquisition of important relationships between the strength of the material evaluated for different loading conditions. Thus, *Piromafo* can be classified as a moderately soft rock with medium stiffness and medium brittleness. Furthermore, the strength and elastic properties of the material decrease in the presence of water in the pores due to the decrease of the surface energy of crack faces and dissolution processes which involve both the neomorphic calcite microcrystals and clay minerals dispersed in the micrite matrix;

*v*) new equations were obtained for estimating compressive strength and tangent modulus by Schmidt hammer rebound values and are quite different from those available in the literature for similar materials.

The data and findings presented in this paper have many practical applications and theoretical implications. They can be useful for better understanding the susceptibility to damage of soft limestones and for planning conservation actions and preventive interventions.

**Funding:** This research was supported by MIUR (Italian Ministry of Education, University and Research) under Grant 2010 ex MURST 60% ''Modelli geologico-tecnici, idrogeologici e geofisici per la tutela e la valorizzazione delle risorse naturali, ambientali e culturali'' (coord.: G.F. Andriani). Work carried out within the framework of the project Interreg III A-"WET SYS B" 2000-2006 (responsible G.F. Andriani), with the financial contribution by the European Community.

**Data Availability Statement:** The data that support the findings of this study are available on request from the corresponding author.

**Acknowledgments:** Thanks are due to Francesco Notarangelo (geologist), Stefano Margiotta (University of Salento, Italy) and Michael Tarullo (Monmouth University, US) for helpful discussions about this paper.

**Conflicts of Interest:** The authors declare no conflicts of interest.

## References

1. Nicotera, P. La Pietra leccese. In *L'Industria Mineraria*; Lega: Faenza, Italia, 1953, anno IV; pp. 449-458.
2. Palmentola, G. Lineamenti geologici e morfologici del Salento leccese. *Quaderni Ricerche del Centro Studi di Geotecnica e di Ingegneria*, 1989, 11, 7–30.
3. Margiotta, S.; Varola, A. Nuovi dati geologici e paleontologici su alcuni affioramenti nel Territorio di Lecce. *Atti della Società Toscana di Scienze Naturali - Memorie*, Serie A, 2004, 109, 1–12.
4. Andriani, G.F.; Walsh, N. Petrophysical and mechanical properties of soft and porous building rocks used in Apulian monuments (south Italy). In *Natural Stone Resources for Historical Monuments*; Přikryl R., Török Á., Eds. The Geological Society, London, Special Publications, 2010; Volume 333, pp. 129–141.
5. Bossio, A.; Foresi, M.L.; Margiotta, S.; Mazzei, R.; Salvatorini, G.; Donia, F. Stratigrafia neogenico – quaternaria del settore nord – orientale della provincia di Lecce (con rilevamento geologico alla scala 1:25.000). *Geologica Romana*, 2006, 39, 63 –88.

 doi:10.20944/preprints202406.0669.v1




6. Arditi, G. *La corografia fisica e storica della provincia di terra d'Otranto*. Tip. Scipione Ammirato, Otranto, Italy,1879; pp. 1-652.
7. Sammarco, M.; Margiotta, S.; Foresi, L.M.; Ceraudo, G. Characterization and provenance of building materials from the Roman pier at San Cataldo (Lecce, Southern Apulia, Italy): A lithostratigraphical and Micropaleonthological approach. Mediterranean Archaeology and Archaeometry 2015, 15(2), 101–112.
8. Tadolini, T.; Tazioli, S.; Tulipano, L. Idrogeologica delle sorgenti Idume. *Geol Appl e Idrogeol* 1971, 6, 41–64.
9. Mongelli, F. Un metodo per la determinazione in laboratorio della conducibilità termica delle rocce. *Boll di Geof Teorica ed Appl* 1968, 10, 51–58.
10. Mongelli, F.; Loddo, M.; Tramacere, A. Thermal conductivity, diffusivity and specific heat variation of some Travale field (Tuscany) rocks versus temperature. *Tectonophysics* 1982, 83(1–2), 33-43.
11. Andriani, G.F.; Walsh, N. Thermal properties and their influence on strength and deformability of calcareous rocks. In *Proceedings of the International Congress Quarry-Laboratory-Monument*, September 26-30, 2000, Pavia, Italy, Calvi G., Zezza U., Eds, pp. 81–90.
12. Dell'Anna, L. La Glauconite nei sedimenti calcarei della Penisola Salentina (Puglia). *Periodico di Mineralogia* 1966, 35, 273 –314.
13. Dell'Anna, L.; Laviano, R. Penisola Salentina: stato delle conoscenze mineralogiche e geochimiche. In: Proceedings of the Congress Conoscenze Geologiche del Territorio Salentino, Lecce, Italia, December 12, 1987, 11, 303–321.
14. Mazzei, R. Età della Pietra leccese nell'area di Cursi-Melpignano (a Sud di Lecce, Puglia). *Bollettino della Società Paleontologica It*. 1994, 33(2), 243–248.
15. Ehlmann, A.J.; Hulings, N.C.; Glover, E.D. Stages of glauconite formation in modern forminiferal sediments. *J. Sediment. Res.* 1963, 33, 87–96.
16. Odin, G.S.; Matter, A. De glauconarium origine. *Sedimentology* 1981, 28, 611–641.
17. Amorosi, A. Detecting compositional, spatial, and temporal attributes of glaucony: a tool for provenance research. *Sediment. Geol.* 1997, 109, 135 –153.
18. Kitamura, A. Glaucony and carbonate grains as indicators of the condensed section: Omna Formation, Japan. *Sediment. Geol.* 1998, 122, 151–163.
19. Kelly, J.C.; Webb, J.A. The genesis of glaucony in the Oligo-Miocene Torquay Group, southeastern Australia: petrographic and geochemical evidence. *Sediment. Geol.*, 1999, 125, 99–114.
20. Clauer, N.; Uysal, I.T.; Aubert, A. Elemental and K-Ar Isotopic Signatures of Glauconite/Celadonite Pellets from a Metallic Deposit of Missouri: Genetic Implications for the Local Deposits. *Geosciences* 2022, 12, 387.
21. Bossio, A.; Mazzei, R.; Monteforti, B.; Salvatorini, G. Nuovo modello stratigrafico del Miocene-Pleistocene inferiore del Salento in chiave geodinamica. In *Proceedings of the 74th National Congress Società Geologica Italiana*, Sorrento, Italia, September 13-17, 1988, 35–38.
22. Balenzano, F.; Margiotta, S.; Moresi, M. Genesi di un deposito glauconitico – fosfatico appartenente ad una unità miocenica del Salento. *Atti Soc Tosc Scienze Nat, Mem*. 2002, Serie A, 109, 1 –16.
23. EN 13373 Natural stone test methods. Determination of geometric characteristics on units. European Committee for Standardization, Brussels, 2020, pp.38.
24. ISRM Suggest methods for the quantitative descriptions of discontinuities in rock masses. *Int. J. Rock Mech. Min. Sci. Geomech. Abstr.* 1978, 15(6), 319–368.
25. ISRM Suggest methods for determining tensile strength of rock materials. *Int. J. Rock Mech. Min. Sci. Geomech. Abstr*. 1978, 15(6), 101–103.
26. ISRM Suggest methods for determining the uniaxial compressive strength and deformability of rock materials. *Int. J. Rock Mech. Min. Sci. Geomech. Abstr.* 1979, 16(2), 135–140.
27. ISRM Suggested methods for determining water-content, porosity, density, absorption and related properties and swelling and slake-durability index properties. Part 1. Suggested methods for determining water-content, porosity, density, absorption and related properties. . *Int. J. Rock Mech. Min. Sci. Geomech. Abstr.* 1979, 16(2). 141–151.
28. EN 1926 Natural stone test methods. Determination of compressive strength. European Committee for Standardization, Brussels, 2006, pp.17.
29. EN 1925 Natural stone test methods. Determination of water absorption coefficient by capillarity. European Committee for Standardization, Brussels, 2000, pp.10.
30. EN 12372 Natural stone test methods. Determination of flexural strength under concentrated load. European Committee for Standardization, Brussels, 2022, pp.18.
31. Andriani, G.F., Walsh, N. Physical properties and textural parameters of calcarenitic rocks: qualitative and quantitative evaluations. *Eng. Geol.* 2002, 67, 5–15.
32. Andriani, G.F., Walsh, N. Fabric, porosity and water permeability of calcarenites from Apulia (SE Italy) used as building and ornamental stone. *Bull. Eng. Geol. Environ.* 2003, 62, 77–84.
33. ASTM D 4404 Standard test method for determination of pore volume and pore volume distribution of soil and rock by mercury intrusion porosimetry. In Annual book of ASTM Standards, 04.08. West Conshohocken, PA, USA, 2018, pp.8.

34. Andriani, G.F., Pastore, N., Giasi, C.I., Parise, M. Hydraulic properties of unsaturated calcarenites by means of a new integrated approach. *Journal of Hydrology*, 2021, 602, 126730.
35. EN 14581 Natural stone test methods. Determination of linear thermal expansion coefficient. European Committee for Standardization, Brussels, 2005, pp.16.
36. Mongelli, F.; Sciruicchio, V.; Walsh, N. Proprietà termiche del Tufo calcareo pugliese. In Proceedings of the International Congress "La Pietra da costruzione: Il Tufo calcareo e la Pietra leccese", CNR-IRIS, Bari, Italia, Bari, May 26-28, 1993 pp 329–349.
37. EN ISO 12571 Hygrothermal performance of building materials and products – Determination of hygroscopic sorption properties. European Committee for Standardization, Brussels, 2013, pp. 25.
38. Aydin, A. ISRM Suggested Method for Determination of the Schmidt Hammer Rebound Hardness: Revised Version. *Int. J. Rock Mech. Min. Sci*. 2009, 46, 627–634.
39. ISRM Suggested Method for Determining Point Load Strength. *Int. J. Rock Mech. Min. Sci. Geomech. Abstr.* 1985, 22(2), 51–60.
40. ASTM C25-19 Standard Test Methods for Chemical Analysis of Limestone, Quicklime, and Hydrated Lime. In Annual book of ASTM Standards, 04.01. West Conshohocken, PA, USA, 2019, pp.40.
41. Choquette, P.W., Pray, L.C. Geologic nomenclature and classification of porosity in sedimentary carbonates. *AAPG Bull.* 1970, 54, 207–250.
42. Dunham, R.J. Classification of carbonate rocks according to depositional texture. In Classification of Carbonate Rocks. American Association of Petroleum Geologists, Ham W.E. Ed., Memoir, 1962, 1, 108–121.
43. Folk, R.L. Practical petrographic classification of limestones. *AAPG Bull.* 1962, 43, 1–38.
44. Geological Society of London. The description of rock masses for engineering purposes: report by the Geological Society Engineering Group Working Party. *Q. J. Eng. Geol.* 1977, 10, 355–388.
45. Přikryl, R. Durability assessment of natural stone. *Q. J. Eng. Geol. Hydrog.* 2013, 46, 377–390.
46. Mindess, S.; Young, J.F.; Darwin, D. *Concrete*. 2nd ed., Prentice Hall, Englewood cliff, NJ, 2002, pp. 644.
47. Zezza, U.; Veniale, F.; Zezza, F.; Moggi, G. Effetti dell'imbibizione sul decadimento meccanico della pietra leccese. In Proceedings of the First International Symposium on the Conservation of Monuments in the Mediterranean Basin, Zezza F. Ed. Bari, June 7-10, 1989, Grafo, Brescia, Italy, 1989, 1, 263–269.
48. Calia, A.; Tabasso, M.L.; Mecchi, A.M.; Quarta, G. The study of stone for conservation purposes: Lecce stone (southern Italy). In Stone in Historic Buildings. Characterization and Performance. Cassar J., Winter M.G., Marker B.R., Walton N.R.G., Entwisle D.C., Bromhead E.N., Smith J.W.N. Eds. The Geological Society, London, Special Publications, 2014, 391, pp 139–156.
49. Pia, G.; Esposito Corcione, C.; Striani, R.; Casnedi, L.; Sanna, U. Coating's influence on water vapour permeability of porous stones typically used in cultural heritage of Mediterranean area: experimental tests and model controlling procedure. (2017) *Progress in Organic Coatings* 2017, 102, 239–246.
50. Mehta, P.K.; Monteiro, P.J.M. Concrete: structure, properties, and materials. McGraw-Hill Professional, 2006, pp. 660.
51. Deere, D.U.; Miller, R.P. *Engineering classification and index properties for intact rocks*. Technical Report, Air Force Weapons Laboratory, New Mexico, AFNL-TR, 1966, 65–116.
52. Lollino, P.; Andriani, G.F. Role of brittle behaviour of soft calcarenites under low confinement: laboratory observations and numerical investigation. *Rock. Mech. Rock. Eng.* 2017, 50, 1863–1882.
53. Andriani, G.F.; Lollino, P.; Perrotti, M.; Fazio, N.L. Incidence of saturation and fabric on the physical and mechanical behaviour of soft carbonate rocks. In Proceedings 53rd U.S. Rock Mechanics/Geomech. Symp., New York City. American Rock Mechanics Association (ARMA), New York. 2019, 1-6, 2044-2048.
54. Rabat, Á.; Cano, M.; Tomás, R. Effect of water saturation on strength and deformability of building calcarenite stones: Correlations with their physical properties. *Constr. and Build. Mat.* 2020, 232, 117259.
55. Singh, R.N.; Hassani, F.P.; Elkington, P.A.S. The application of strength and deformation index testing to the stability assessment of coal measures excavations. In Proceedings 24th US Symp. On Rock Mech. Texas A and M Univ. AEG, Balkema, Rotterdam, 1983, pp. 599–609.
56. O' Rourke, J.E. Rock index properties for geoengineering in underground development. Min. Eng. 1989, 106– 110.
57. Katz, O.; Reches, Z.; Roegiers, J.C. Evaluation of mechanical rock properties using a Schmidt Hammer. Int. J. Rock Mech. Min. Sci. 2000, 37, 723–728.
58. Yagiz, S. Predicting uniaxial compressive strength, modulus of elasticity and index properties of rocks using the Schmidt hammer. *Bull. Eng. Geol. Env.* 2009, 68, 55–63.

 doi:10.20944/preprints202406.0669.v1



59. Aydin, A.; Basu, A. The Schmidt hammer in rock material characterization. *Eng. Geol.* 2005, 81, 1–14.
60. Andriani, G.F.; Germinario, L. Thermal decay of carbonate dimension stones: fabric, physical and mechanical changes. *Env. Earth. Sci.* 2014, 72(7), 2523–2539.